

## PARAMETER OPTIMIZATION OF MULTI-LEVEL DIFFRACTION GRATINGS

MATĚJKA Milan<sup>1</sup>, KOLAŘÍK Vladimír<sup>1,\*</sup>, HORÁČEK Miroslav<sup>1</sup>, KRÁL Stanislav<sup>1</sup>

<sup>1</sup> *Institute of Scientific Instruments of the CAS, Brno, Czech Republic, EU*  
[vladimir.kolarik@isibrno.cz](mailto:vladimir.kolarik@isibrno.cz)

### Abstract

Originally, the e-beam lithography (EBL) is a technique for creating high-resolution black and white masks for the optical lithography. Multi-level relief structures can be also prepared using EBL patterning. Their preparation is based on the image patterning with a gradient of exposure doses. Large-area multi-level structures can be effectively prepared using the electron beam pattern generator with a variable shaped beam. We present several writing strategies. Basically, the main writing strategy uses one stamp (i.e. one elementary exposure of the shaped electron beam) per one elementary area with the same exposure dose. This simple approach is fast and flexible, however it does not guarantee optimal results. The main problem is an imperfection of the stamps (size, shape, and homogeneity). Advanced algorithms are based on multiple exposure of the same elementary area, the total local exposure dose is a sum of several different elementary exposures (stamps). Using these algorithms, a smoother surface of the structure can be achieved. On the other hand, the writing speed is considerably decreased. Tradeoff between the achieved parameters and the writing speed is discussed for selected set of writing strategy algorithms.

**Keywords:** E-beam pattern generator, variable shaped beam, grayscale lithography, multi-level grating

### 1. INTRODUCTION

Multi-level and blazed diffraction grating are one of strong security features included in diffractive optical variable image devices for optical document security applications [1]. Such high quality asymmetrical gratings are difficult to be prepared by optical methods, usually some kind of advanced lithography techniques is to be adopted. The e-beam lithography is one of suitable techniques. However, the realization of high quality blazed profile with the surface roughness in the 10-nm range is not easy, mainly if the high writing speed is required. The multi-level gratings are one of the typical patterns where the resolution of the shaped beam pattern generator is adequate and its writing speed is better than that of the Gaussian type pattern generator [2], especially when the number of levels increases. Several aspects must be considered during the patterning of large-area samples (several square centimeters or inches) of such kind of gratings.

- The exposure process is composed of a series of elementary variable-size exposures (stamps). The requirements to the homogeneous current distribution with the stamps are high, thus appropriate methods for adjustment and check of this homogeneity is important [3], [4].
- The choice between two available writing modes of the BS600 pattern generator, the standard mode (maximum stamp size is 6.3 microns, lower current density), the TZ mode [5] (technology zoom mode, maximum stamp size 2.1 microns, higher current density).
- The quality of blazed gratings profile is deteriorate by the proximity effect if the appropriate correction methods [6], [7], [8], [9] are not adopted; this problem becomes obviously more important as the grating period decreases.
- Homogeneity of large-area grating is also related to the stamp homogeneity over the exposure field [10].

## 2. METHODS

We present four writing strategies represented by four different algorithms, see **Figure 1**. The basic approach (algorithm I) uses approximately square stamps, their size is derived from grating period and number of levels by which the blazed profile is approximated. Dosing of individual stamps is set such that the dose gradient of required number of exposure levels is achieved. The drawback of this approach is in the border between adjacent stamps; usually, small discrepancies of stamp dimensions and the current uniformity of individual stamps makes some differences in locally absorbed dose, these differences locally modify the flatness of the multi-level relief (**Figure 2**) and decrease the optical quality of diffraction gratings. The algorithm II uses exposure stamps of minimum size ( $\sim 200$  nm); the stamp induced relief modulation is moderated and its spatial frequency is transposed to higher values; this approach however decreases importantly the writing speed. Two smoothing algorithms are proposed. They use the realization of dose gradients by integration of doses of several overexposed stamps. While the algorithm IIIA performs the relief smoothing in one direction (perpendicularly to the grating lines, the algorithm IIIB performs the smoothing in both X and Y directions [11].

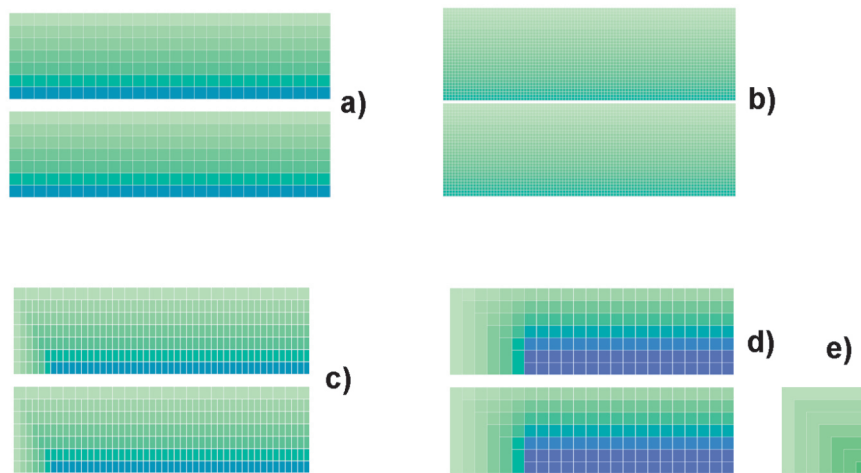


**Figure 1** Schematic representation of writing algorithms: basic algorithm I (a); minimum-size stamps algorithm II (b); smoothing algorithm in one direction IIIA (c); smoothing algorithm in two directions IIIB (d); and its basic sub pattern (e)

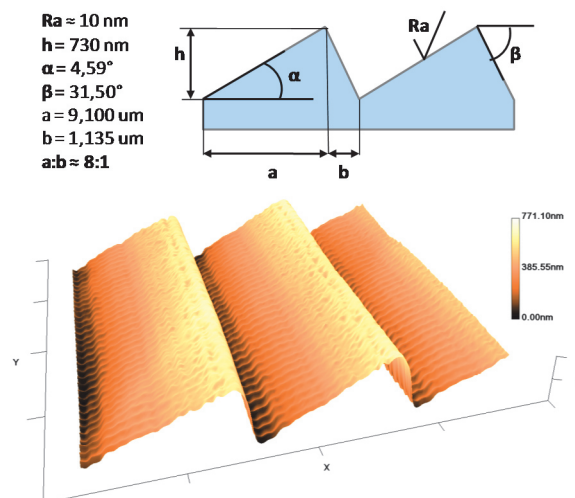


**Figure 2** AFM scan of the 16-level grating; period  $\Lambda = 10 \mu\text{m}$ , depth  $h \sim 730$  nm

### 3. EXPERIMENT

A sample for comparison of various algorithms using the e-beam writer BS600 was prepared. The test structure is composed of 22 square areas  $1\text{ mm} \times 1\text{ mm}$ . Each square is filled with a multi-level grating with 10-micron period (periodicity of lines). Three different algorithms were used to generate the gratings, denoted I, IIIA, and IIIB in the text above. The testing sample layout is depicted in **Figure 3**. **Table 1** summarizes basic parameters of the gratings.

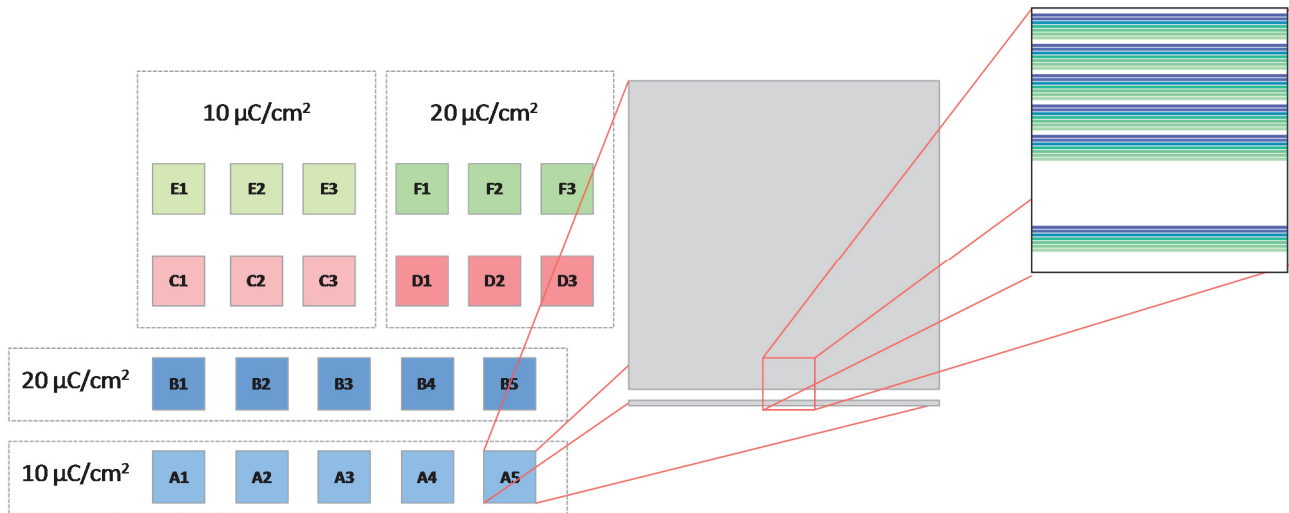


**Figure 3** Layout of the testing motifs, see details in the text and in **Table 1**

**Table 1** Number of levels, testing motifs from **Figure 3**

motif	dose [ $\mu\text{C}/\text{cm}^2$ ]	algorithm	number of levels				
			variant 1	variant 2	variant 3	variant 4	variant 5
A	10	I	50	32	25	16	8
B	20	I	50	32	25	16	8
C	10	IIIA	8	16	32		
D	20	IIIA	8	16	32		
E	10	IIIB	8	16	32		
F	20	IIIB	8	16	32		

The testing motifs were exposed using the e-beam writer with a rectangularly shaped beam Tesla BS600 (acceleration voltage 15 kV). As the first step it was necessary to measure the uniformity of the current distribution of the electron beam stamps in a Faraday cup [3]. Next, prior to the grating motifs exposure, we exposed technological testing structures for checking the adjustment of the BS600 electron optical system. The testing motif data was recorded to PMMA layer on Si wafer. We used a monolayer PMMA with a molecular weight  $MW \approx 350\text{k}$ , and the thickness  $w \approx 2000\text{ nm}$ . The given molecular weight was chosen because of the possibility of achieving required shape and slope of the sensitivity curve (low resist contrast).

The development of the test sample after exposure was carried out in a spin processor by application of a developer - n-amyl-acetate (nAAc) with concentration of 98.5 %. The development was performed gradually in five steps, with an overall time of 450 seconds. After each step we inspected the recorded grating structures

and technological tests with an optical microscope. The development was terminated when the test area with exposure dose of  $40 \mu\text{C}/\text{cm}^2$  was fully cleared from the resist to the silicon surface. This dose value corresponds to the depth of the grating motifs of 200-250 nm and 400-500 nm, for the maximum grid dose of  $10 \mu\text{C}/\text{cm}^2$  and  $20 \mu\text{C}/\text{cm}^2$  respectively. The grating depth of 200-250 nm is suitable for optical evaluations (diffraction efficiency measurements).

After the development step, the surface relief of sample grids structures was measured using an atomic force microscope (AFM), type Nano-R from Pacific Nano Technology. Data analysis and the evaluation of profile roughness was performed using the software tool NanoRuler+.

#### 4. RESULTS AND DISCUSSIONS

Evaluation and benchmarks for the comparison of recorded structures were selected as follows: surface quality (surface roughness  $R_a$ ), optical performance of the gratings (diffraction grating efficiency  $\eta$ ), exposure time of a particular pattern (writing speed). Hereafter, we present for the purpose of compactness only the results that were measured on the patterns with the lower exposure dose ( $10 \mu\text{C}/\text{cm}^2$ ), i.e. all variants of patterns A, C and E.

Let us start with the comparison of the writing speed. The fastest writing algorithm in this respect is the basic writing method (A1-A5), as expected. According to the assumptions the smoothing algorithm (C1-C3 and E1-E3) requires longer computational and exposure time but, with today's computational performance of typical personal computers, it remains within acceptable limits.

**Figure 4** shows AFM profile scans of the implemented grating with selected writing strategies. Two set of profiles (8-level structures and 16-level structures) are presented. The grating prepared with the basic unoptimized writing strategy is plotted in blue (A5, A4); the two reliefs resulting from the optimized strategies are plotted in red (C1, C2), and in green (E1, E2). It was observed that the higher degree of relief approximation (a higher number of levels or steps) implies the more smoothing profile and the reduction of step artifacts. The rounding of profile grid is primarily due the nonlinear dependence of sensitivity curves for a given combination of resist and developer. In the case of the basic writing algorithm, transition zones between adjacent levels are more pronounced for the gratings recorded with a higher number of levels (compare lines A5 and A4 in **Figure 4**). Considerable enhancement of the surface roughness is seen in the direction perpendicular to the grating lines for both types of smoothed structures (IIIA and IIIB), see **Figure 5**.

The average roughness  $R_a$  is evaluated from the optically active area of the grating surface. The result is depicted in **Figure 6**, where the  $R_a$  dependency on the number of levels  $N$  of the recorded gratings is plotted. The result implies that the surface roughness is significantly reduced in case of both smoothing writing strategies (IIIA and IIIB, lines C1-C3 and E1-E3 respectively). Regarding the smoothing algorithms (C1-C3 and E1-E3) it holds that with the increasing number of levels there is a strengthening of the positive effect of surface roughness reduction. Conversely, regarding the basic unsmoothed structure (A1-A5) the surface roughness seems to increase with the increasing number of levels; it is probably caused by the increasing amounts of transitions between adjacent stamps that cause inhomogeneity in absorbed energy.

The final phase of the evaluation was the measurements of the diffraction gratings efficiency. Prior to the measurements the resist layer was sputtered by a silver layer with thickness of about 100 nm. Then, the measurements were performed on the apparatus consisting of laser source ( $\lambda = 650 \text{ nm}$ ), detector, luxmeter with cosine filter and angularly adjustable holder. Measurements took place at approximately normal incidence of the laser beam. We measured the intensity of up to the 4th diffraction order (-4 to +4, including the zero order, i.e. the reflection). It was always necessary to measure the intensity of the laser reflection from the unpatterned silver layer. The measurement results are presented in the graph of **Figure 7**. One can observe relatively high efficiency of the first diffraction order, which is about 60-80 % in all cases.

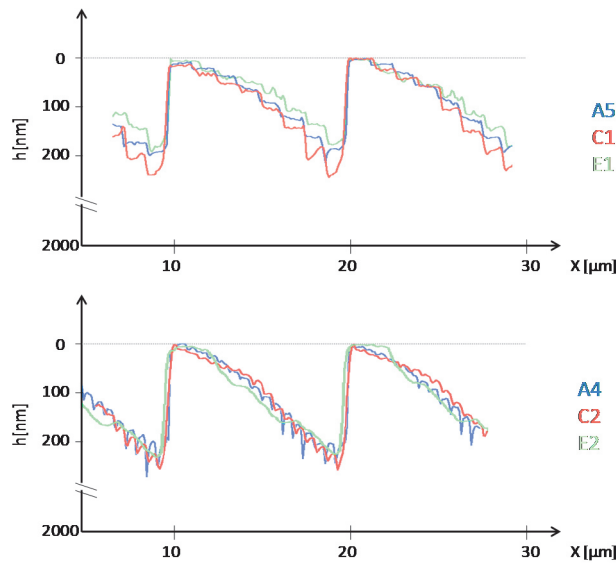


**Figure 4** Comparison of the measured multi level grating profiles: 8-level approximation with step width of 1250 nm and step height of ~ 36 nm (above); 16-level approximation with step width of 600 nm and step height of ~ 18 nm (bottom)



**Figure 5** Comparison of the smoothing algorithms results: AFM scan along the grating line

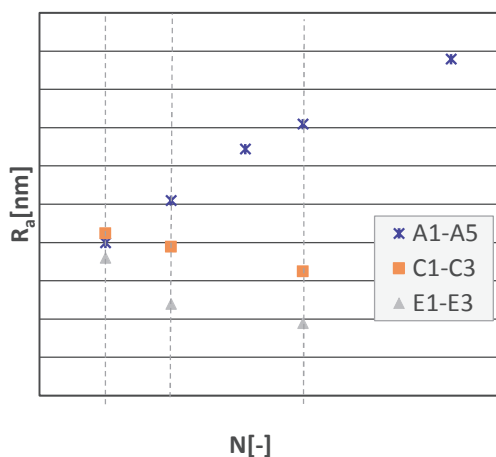


**Figure 6** Evaluation of the average surface roughness ( $R_a$ ) measured at the optically active surface of the gratings

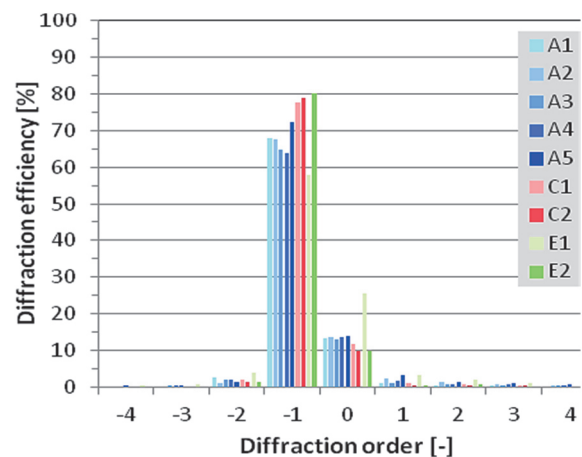


**Figure 7** Measured diffraction grating efficiency for the diffraction gratings orders  $m \in \langle -4, 4 \rangle$ , measured by red laser ( $\lambda = 650 \text{ nm}$ )

## 5. CONCLUSIONS

We presented several algorithms for writing strategy of multi-level relief gratings. New algorithms are based on the dose gradient that relies on the exposure dose accumulation during multiple exposures. The e-beam writer with a shaped beam BS600 was used for the patterning of sample structures. The analysis of results shows the positive effect of the new algorithms on the optical properties of the prepared relief gratings. The related ongoing work is continued in two directions. First, the optimization of the presented algorithms is on the way such that they are able to handle both the sensitivity curve nonlinearities and the proximity effect correction for short-period gratings. Second, we are focused on the optimization of the algorithms which are based on the minimum-size stamps. The achieved results are very useful both in the field of diffractive optically variable image devices and in the area of light beam processing in the visible region.

## ACKNOWLEDGEMENT

***The research was partially supported by the MIT CR projects FR-TI1/574 and FR-TI1/576, by the TACR project TE 01020233, by MEYS CR (LO1212), its infrastructure by MEYS CR and EC (CZ.1.05/2.1.00/01.0017) and by CAS (RVO:68081731).***

## REFERENCES

- [1] RENESSE, R. L. van, *Optical Document Security, 3rd edition*, Boston/London: Artech House (2005), 386 pages, ISBN 1-58053-258-6.
- [2] HORÁČEK, M. *et al.*, Exposure Time Comparison between E-Beam Writer with Gaussian Beam and Variable Shaped Beam. In *NANOCON 2014: 6th Int'l Conference Proceedings*. Ostrava: TANGER, 2014, pp. 252-256.
- [3] BOK, J. *et al.*, Modified knife-edge method for current density distribution measurements in e-beam writers. *Journal of Vacuum Science & Technology B*. Vol. 31, no. 3 (2013), pp. 031603:1-6.
- [4] BOK, J. *et al.*, Measurements of current density distribution in shaped e-beam writers, *Microelectronic Engineering*, Vol. 149, 5 January 2016, pp. 117-124.
- [5] KOLAŘÍK, V. *et al.*, E-Beam Pattern Generator BS600 and Technology Zoom. In *NANOCON 2012: 4th International Conference Proceedings*. Ostrava: TANGER, 2012, pp. 822-825.
- [6] URBÁNEK, M. *et al.*, Shaped E-beam Nanopatterning with Proximity Effect Correction. In: *NANOCON 2012, 4th International Conference Proceedings*. Ostrava: TANGER, 2012, pp. 717-722.
- [7] URBÁNEK, M. *et al.*, Variable Shape E-Beam Writing: Proximity Effect Simulation and Correction of Binary and Relief Structures. In *39th International Conference on Micro and Nano Engineering MNE2013: Book of Abstracts*. Cambridge: University of Cambridge, 2013, p. 582.
- [8] MATĚJKA, M. *et al.*, Variable Shape E-Beam Lithography: Proximity Effect Simulation of 3D Micro and Nano Structures. In: *NANOCON 2012, 4th Int'l Conference Proceedings*. Ostrava: TANGER, 2012, pp. 729-732.
- [9] URBÁNEK, M. *et al.*, Determination of Proximity Effect Forward Scattering Range Parameter in E-Beam Lithography. In *Recent Trends in Charged Particle Optics and Surface Physics Instrumentation: 12th Int'l Seminar Proceedings*, Brno: ISI ASCR, 2010, pp. 67-68.
- [10] KOLAŘÍK, V. *et al.*, Large-Area Gray-Scale Structures in E-Beam Writer versus Area Current Homogeneity and Deflection Uniformity. In *Proceedings of the 15th International Seminar on Recent Trends in Charged Particle Optics and Surface Physics Instrumentation*. Brno: ISI CAS, 2016, pp. 26-27.
- [11] MATĚJKA, M., Submicron Structures with Deep Relief - Technology of Preparation, Brno, 2016, Ph.D. Thesis (*in Czech*), Brno University of Technology, Faculty of Electrical Engineering and Communication Technology.